Reduced-order models for assessing Demand Response with heat pumps – insights from the German energy system

Evelyn Sperber [a] *, Ulrich Frey [a], Valentin Bertsch [b]

[a] Department of Energy Systems Analysis, Institute of Engineering Thermodynamics, German Aerospace Center (DLR), Pfaffenwaldring 38-40, 70569 Stuttgart, Germany

[b] Chair of Energy Systems and Energy Economics, Ruhr-Universität Bochum, Universitätsstraße 150, 44801 Bochum

* Corresponding author. E-mail address: evelyn.sperber@dlr.de (E. Sperber)

Abstract

Heat pumps are regarded as one promising option for Demand Response (DR) in renewable-dominated energy systems. By activating the structural thermal mass of buildings, power consumption of heat pumps can be decoupled from heat demand. Assessing the system-wide DR potential from heat pumps requires adequate models to account for the thermal response of the building stock to flexible operation. In this study, reduced-order thermal response models of twelve representative German building types in three insulation states are provided based on grey-box modeling. The identified models reveal a good compromise between accuracy of the simulated indoor temperature (RMSE of on average 0.6 °C) and computational cost (acceleration by factor 250) compared to the complex building simulation software TRNSYS. Furthermore, these reduced-order models are employed in a case study to estimate the technical DR potential of heat pumps by passive storage at specified ambient conditions. Extrapolated to the future stock of German single family houses, the maximum shiftable heat pump load adds up to 57 GW_{el}. The structural thermal mass of the building stock enables maximal 300 GWh_{el} of electrical energy to be discharged at a very cold winter day and 185 GWh_{el} to be charged at milder temperatures.

Keywords: Demand Response; Heat pumps; Passive storage; Grey-box modeling; Reduced-order models

1 Introduction

1.1 Motivation

Growing climate and environmental concerns, significant cost reductions and limited availability of fossil fuels have promoted renewable energies as a pillar of energy strategies of countries worldwide [1]. Due to the intermittent nature of most renewables, future energy systems require additional flexibility in order to balance supply and demand. Flexibilities that are commonly discussed are, among others, grid extension [2], energy storage [3], flexible thermal generation [4] and Demand Response (DR) [5].

One promising DR option is to operate heat pumps for space heating flexibly. This option has received increasing attention as a measure to cost-effectively integrate intermittent renewables [6]. In smart grids, heat pumps can be thermostatically controlled depending on the requirements of the power sector. Such a disconnection of power consumption and heat demand does not necessarily rely on investments in separate thermal storage tanks (i.e. active storage). Instead, it is enabled by activating the structural thermal mass of buildings (hereinafter also referred to as passive storage) [7]. Thus, the internal temperature is varied within certain comfort limits in order to store or withdraw energy.

Since heat pumps are anticipated to play a major role in decarbonized energy systems [8], significant loads can be expected in the future for the building sector that might be available for DR. In Germany, for example, about 40 to 85 % of the heat demand of buildings could be generated by electric heat pumps by 2050, corresponding to an electricity demand for space heating of up to 200 TWh [9]. It is therefore worth analyzing the effects of this DR on the energy system in detail.

1.2 State of the art of system-wide assessment of DR with heat pumps

A challenge to be overcome in the system-wide assessment of DR with heat pumps is the adequate consideration of the thermal response of the building stock to flexible heat pump operation, including passive storage. Different approaches have been described in the literature and are characterized in the following paragraphs.

One approach for representing building thermodynamics within energy system models in the context of DR with heat pumps is to couple complex thermodynamic building simulation models to energy system models. An exemplary study from this field is presented by Papaefthymiou et al. [10]. The

58 authors perform detailed thermodynamic simulations of representative building types and incorporate
59 the thermal behavior of the building stock in a high-level model of the German power market. This
60 allows evaluating system effects of flexible heat pumps by use of passive storage for the years 2020
61 and 2030. However, the application of detailed building simulation models appears to be too
62 computationally expensive in order to simulate energy system transitions with a time horizon of usually
63 30 to 50 years.

64 A different approach to study DR with heat pumps at system level is to take heat demand as
65 exogenous model input data and disregard endogenous building thermodynamics. While being
66 computationally efficient, this comes at the expense of the accuracy of the building thermal response
67 to flexible heat pump operation. For instance, some studies from this area consider the thermal mass
68 of buildings as a generic storage [11,12], partly limiting load shifting to a fixed period of 2 h [11].
69 However, several other building-level studies show that the passive storage potential is highly
70 dependent on ambient conditions [13] and that time shifts can last from 2 h to more than 24 h
71 depending on the insulation standard [14,15]. Further studies only consider water storage tanks for
72 providing flexibility and neglect passive storage [16–18]. This is problematic insofar as other studies
73 find that passive storage can maintain thermal comfort in well-insulated buildings during DR
74 interventions [19] and should be preferred to active storage from a cost-benefit point of view [7].

75 As a bridge between accuracy of building thermodynamics on the one hand and computational
76 efficiency on the other hand, a third approach to assess DR with heat pumps is the application of
77 linear state space models of building thermodynamics. Kotzur [20], for instance, integrates a single-
78 state model of thermodynamics of different building types into a cost optimization model of the
79 German energy sector. However, the accuracy of single-state models of building thermodynamics is
80 questioned by others [21,22]. More detailed linear state space models of building thermodynamics of
81 different building types are applied in Hedegaard and Balyk [23], who study prospective benefits of
82 flexible heat pumps for the Danish energy system. Yet, they simplify by neglecting solar transmission
83 and by assuming a constant coefficient of performance for heat pumps. Further studies from this area
84 are Baeten et al. [24] and Arteconi et al. [25], who find positive effects of DR with heat pumps on the
85 Belgian energy market. The state space models employed in both studies emulate complex building
86 thermodynamics, but only represent a single building type. As studies at the level of individual
87 buildings show, this is a shortcoming since the DR potential varies significantly depending on the

building construction and energetic standard [14]. The most detailed system-level study known to us using linear state space models of building thermodynamics is Patteeuw et al. [26], who consider 36 representative Belgian building types of different renovation levels in their study on DR with heat pumps in Belgium. In this manner, the authors are able to assess CO_2-abatement cost of heat pumps subject to building characteristics and heating systems.

Linear state space models of building thermodynamics are a suitable approach to assess DR with heat pumps at the level of energy systems, because they a) allow the inherent consideration of passive storage and b) come at low computational cost, which is why they can be integrated into more complex energy system models [27]. It is therefore useful to take a closer look at them.

For the development of such models, one challenge is their parametrization. The parameters of the models of two of the studies mentioned above [20,23] are based on literature values, e.g. building typology data. However, both studies do not provide a validation of the resulting dynamic building thermal behavior. Studies [24–26], instead, incorporate validated linear state space models based on grey-box modeling. This method is described in detail in the following section.

1.3 Grey-box modeling of building thermal response

Grey-box models combine a simplified physical description of a system's behavior with data to estimate the model parameters. They are thus a hybrid of white-box models which are purely based on a theoretical and complex system description, and black-box models that only rely on measured input and output data of a system. Grey-box models are commonly represented by a set of stochastic differential equations in state space form that describe the system dynamics based on prior physical knowledge [28]. For time-invariant systems, the system equation is denoted as follows:

$$dX(t) = A(\theta)X(t) + B(\theta)U(t) + K(\theta)d\omega \quad \text{Eq. 1}$$

where X(t) is the state vector, U(t) is the input vector, A is the system matrix, B is the input matrix, K is the noise matrix and ω is a Wiener process. The measured outputs of the system are given by the observation equation:

$$Y(t) = C(\theta)X(t) + D(\theta)U(t) + \varepsilon \quad \text{Eq. 2}$$

where C is the output matrix, D the feedforward matrix and ε is the measurement error. The vector of unknown parameters Θ of the system is estimated by statistical methods.

Grey-box modeling is employed in several studies to identify appropriate models of building thermodynamics [29]. Most of them focus on model predictive control. In the building context, system equations are frequently represented by lumped parameter models based on RC-networks in electric analogy [30]. Thereby, assumptions about thermodynamics are transformed into a network of lumped thermal resistances (R) and capacitances (C). In some publications, measurement data of existing buildings are used to estimate the parameters of the models, while detailed building simulation software is utilized to generate data in other studies.

Table 1 summarizes the findings of the relevant literature in the context of grey-box modeling of thermal response of entire buildings. In case several RC-models are evaluated in a study, the model that generates the most accurate predictions is given. Otherwise, the notation of the only model considered is shown. The model notation is based on the number of R and C used in the system equation. If available, the widely used error measure, root mean square error (RMSE) for prediction of the indoor temperature compared to reference data is given with the corresponding temporal prediction horizon.

Table 1: Literature review on grey-box modeling of thermal response of entire buildings. Data origin: M = Measurements, S = Simulation model

Study	Building type(s)	Building location	Data origin	(Optimal) model	RMSE	Prediction horizon
Coley and Penman 1992 [31]	School building	United Kingdom	M	3R2C	≈ 1.0 °C	≈ 40 days
Bacher and Madsen 2011 [32]	Research building	Denmark	M	4R4C		n.a.
Hazyuk et al. 2012 [33]	Detached house	n.a.	S	4R2C		n.a.
Reynders et al. 2014a [34]	Old detached house / New detached house	Belgium	S	6R4C / 8R5C	≈ 0.5 - 1.0 °C	2 days - 1 week
Reynders et al. 2014b [35]	15 typical single family houses	Belgium	S	13R9C	≈ 0.2 - 1.0 °C	2 days - 1 week
Berthou et al. 2014 [36]	Office building	France	S	6R2C		n.a.
Fux et al. 2014 [37]	Alpine lodge building	Switzerland	M	6R4C	0.4 °C	12 days
Reynders et al. 2015 [38]	New detached house with variation of heating system	Belgium	M	1R1C - 6R4C	1-5%	1 week
Dimitriou 2016 [39]	11 residential buildings	United Kingdom	M	3R2C	1.0 °C	8 weeks
Harb et al. 2016 [40]	Office building	Germany	M	4R2C	0.2 °C	8 weeks
Fonti et al. 2017 [41]	Office building	Italy	M	3R2C	0.4 °C / 0.9 °C	1 hour / 3 hours
Massano et al. 2019 [42]	Industrial building	n.a.	S	1R1C	0.4 °C	24 hours

131 The reviewed studies reveal that grey-box modeling generates valid approximations of the thermal
132 response of buildings. Some studies find that models with two capacitances can sufficiently capture
133 the thermodynamics of buildings, while others report that modeling up to five capacitances improves
134 the model performance. For short-term prediction (up to 48 hours), RMSE of less than 0.5 °C are
135 identified in some studies, while longer prediction horizons (one week or more) tend to increase the
136 RMSE to about 1 °C.

137 As apparent from Table 1, grey-box modeling of thermal response has so far mainly been presented
138 for specific buildings. One important exception is Reynders et al. [35], who develop grey-box models
139 for a typology of Belgian single family houses. The typical buildings that are considered are
140 representative for the Belgian building stock and thus enable nationwide system analyses by
141 aggregation. Their models are e.g. applied by Patteeuw et al. [26], who assess interactions between
142 heat pumps in buildings and the Belgian energy market (see section 1.2).

143 **1.4 Research gaps**

144 To the best of our knowledge, grey-box modeling of building thermal response has not yet been
145 presented for German residential building types. This is a shortcoming, because future system
146 analyses on DR with heat pumps in the German energy sector will require coherent models of the
147 thermodynamics of German building types. The models of the Belgian building stock developed by
148 Reynders et al. [35] are not perfectly adequate for application in German system analyses for the
149 following reasons: first, building characteristics differ across European countries with regional
150 distinctions in the way of construction [43]. Second, building energy regulations are and have been
151 different in Germany and Belgium. Therefore, energy standards for the various building construction
152 periods differ (compare [44] and [45]). Third, the RC-models of the Belgian building stock are
153 extensive two-zone models with separate RC-formulations for a day- and a night-zone of each building
154 type. Even though each of the separate models shows a very good prediction of the indoor
155 temperature, the combined model has a somewhat lower quality. Moreover, the combined model has
156 nine capacitances which means that computation time is higher by a factor 15 or 20 than that of
157 models with only two or three capacitances (see section 3.1.2).

158 As a consequence of the lack of adequate reduced-order thermodynamic models of representative
159 German building types, there is also a gap of knowledge regarding the heat pumps' DR potential
160 through passive storage for the German building stock. While previous studies have already presented

system-level studies on DR with heat pumps in Germany, particularly the role of passive storage remains unclear due to the insufficient thermodynamic description of representative buildings within the applied energy system models in those studies [11,12,16–18,20], or is not transferable for simulations over several years because of a too complex model coupling [10] (compare section 1.2) .

1.5 Objective and scope of this study

We therefore aim to close this gap by providing tailor-made models with a high predictive power that are representative for the majority of the German building stock while having low computational cost. These models incorporate building heterogeneity, weather as well as user preferences in order to sufficiently reflect the thermal response of buildings to flexible heat pump operation. To this end, we follow the approach of Reynders et al. [35], with the following distinctions: On the one hand, we adapt the data needed for grey-box modeling on a variety of representative German building types. On the other hand, we use less complex, computationally highly efficient RC-formulations which facilitate the integration into complex models of large energy systems. To demonstrate the efficiency of the models, we implement them in a case study to estimate the technical potential of heat pumps for DR by passive storage for the future stock of single family houses in Germany.

The focus of our study is on Germany for the following reasons: Germany is important to study in more detail for questions concerning energy transition, since it makes up about 20 % of the final energy consumption in households of the EU-28 [46]. Moreover, countries differ markedly in heating technologies – while heat pumps are regarded as key technology for the German heating market [9], other countries like Denmark rely on alternative heating technologies, like district heating [47]. Hence, heat pumps could provide a large DR potential for the German energy market.

The remainder of this study is structured as follows. Chapter 2 describes the methodology for identifying reduced-order models of the thermal response of German building types and for their application in a case study. Chapter 3 presents and discusses the results of our grey-box modeling approach as well as the DR potential of the German stock of single family houses. The final chapter concludes and states limitations of our work.

2 Methodology

In this study, reduced-order models of the thermal response of German building types are developed (section 2.1) and then applied in a case study in order to calculate the DR potential by passive storage (section 2.2). The methodological procedure for these two tasks is described separately below.

2.1 Grey-box modeling of thermal response of German building types

2.1.1 Selection and characterization of building types

In order to map thermodynamics of all buildings in Germany, representative building types are modelled. These building types approximate the German housing stock by aggregation. In this study, the German building typology of 2015 [45] is used as the central source for the structural and energetic characterization of representative residential buildings. The typology was developed as part of the European projects TABULA and EPISCOPE, which provided a harmonized structure to classify building types at European level and created building archetypes based on statistical analyses of large building samples [43].

The German building typology groups the German housing stock into building sizes (single family houses (SFH), multiple dwellings etc.) and construction periods according to their energy-relevant characteristics. For each class, a real example building is described whose properties are representative for the respective building class. The typology provides information on building geometrics, construction materials, heat transfer coefficients of building components, measures for thermal insulation and the calculated heat demand for every building type.

The focus of our study is on SFH which represent 66 % of the German residential building stock [48] and which are the most relevant application of heat pumps [49]. In the German building typology, SFH are described by twelve types. Their distribution in Germany is given in Table 2.

Table 2: Stock of SFH according to the German building typology [45]

Code of building type	Construction period	Heated living area in m²	Building stock in thousands
SFH A	< 1859	199	330
SFH B	1860 - 1918	129	966
SFH C	1919 - 1948	275	1,131
SFH D	1949 - 1957	101	859
SFH E	1958 - 1968	110	1,509
SFH F	1969 - 1978	158	1,507
SFH G	1979 - 1983	196	704
SFH H	1984 - 1994	137	1,160
SFH I	1995 - 2001	111	1,035
SFH J	2002 - 2009	133	907*
SFH K	2010 - 2015	160	494*
SFH L	> 2016	160	258**

* numbers derived from Federal Statistical Office [50]
** stock end of 2018 [50]

For each building type, three variants depending on the insulation state are defined in the typology. In the remainder of our study, these variants are labeled as follows: the code “Var1” refers to the original condition at construction of the building. “Var2” stands for the building condition after a conventional renovation with moderate insulation of the building shell and window replacement with two-panes glazing. Finally, “Var3” describes the building condition after deep renovation with high insulation and three-panes glazing. The thermal characterization of the building types can be found in Appendix A, Table A.1.

2.1.2 Creation of a reference dataset

For parameter estimation, data on the thermal response of the buildings types are required. Real measurement data of these building types are not available. In our study, they are determined on the basis of a complex physical building model – a white-box model – with the simulation software TRNSYS 17 [51] instead.

In TRNSYS, a project is set up by connecting individual components of a thermal system. Each component is described mathematically. For the central component of our study, building, the extensive multizone building model of TRNSYS is used. For parametrization of each building model in TRNSYS, geometric and further energy-relevant data from the building typology is used. In addition, the following assumptions and simplifications are made:

- Buildings are approximated by a single thermal zone and are modeled as rectangular blocks with equal orientations across cardinal directions.

- In line with the TABULA calculation method for heating demand [45], internal heat gains are held constant at a rate of 3 W/m² and a shading factor of 0.6 is used. The set point temperature is 20 °C with a night setback to 18 °C.
- Air change rate is constant at 0.4/hr (in line with TABULA) for Var1 and Var2 and at 0.1/hr for Var3. The low air change rate for Var3 is based on the fact that no mechanical ventilation system with heat recovery is simulated with TRNSYS that would otherwise maintain hygienic air exchange (TABULA assumes 80 % heat recovery).
- Internal walls and furniture are not modelled explicitly. Instead, they are considered by increasing the capacitance of the internal air by a factor of 5 [34].

Assumptions regarding the heat distribution system for each building type can be found in Appendix A, Table A.2. Since the focus of grey-box modeling in our study is on the building thermal response to a given heat input, heat pumps are not modeled explicitly. Instead, a simple boiler is assumed. The maximum heat load of each building type is calculated by TRNSYS for a minimum ambient temperature of -14 °C and a set point temperature of 22 °C. The nominal powers of the boilers are set accordingly. A weather-compensated heating control is implemented in TRNSYS. For building types A to I, radiative and convective heating power is calculated in an external radiator model which is connected to the building model. Buildings J to L, on the other hand, have underfloor heating, which is already integrated in the building model.

Two simulation runs with different weather data are carried out for each building type. The first runs provide a plausibility check of the TRNSYS models by comparing the resulting annual heating demands of the building types to data from TABULA. For this purpose, the test reference year 2010 of Potsdam [44], which serves as a reference climate for Germany [45] and also for the TABULA calculations, is used. Annual heating demands derived from TRNSYS and TABULA are given in Figure 1. The average deviation between TABULA and TRNSYS heating demand is 8 %. This represents a good agreement against the TABULA calculations. While TRNSYS performs dynamic simulations in high temporal resolution, TABULA calculates the heat demand statically according to the simplified heating period balance of EN ISO 13790. Moreover, the deviation is in a similar range as reported by other authors who compare heat demands derived from transient simulations with typological data [52].

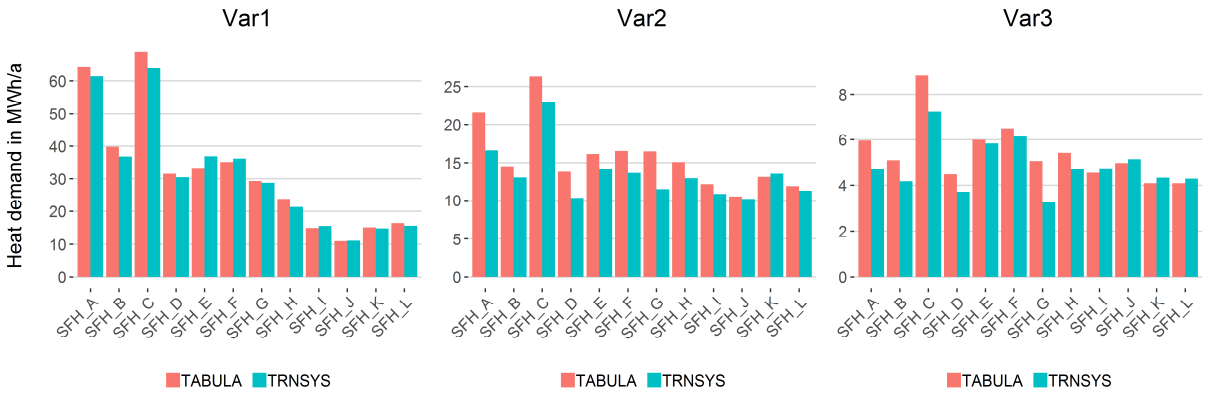


Figure 1: Annual heating demand, calculated by TABULA vs. simulated by TRNSYS

The second simulation runs serve to provide data for the grey-box modeling. They rely on different weather data, because problems have been reported with regard to the use the test reference year of 2010, especially concerning solar radiation data [53]. Instead, weather data of Meteonorm [54] of Stuttgart, Germany is used (data shown in Appendix B).

Transient simulations are carried out with a time-step of six minutes. The following time series are derived from TRNSYS for grey-box modeling:

- Indoor air temperature
- Heating power (i.e. heat injected into radiators or underfloor heating)
- Processed solar radiation

2.1.3 RC-model formulation

In accordance to Bacher and Madsen [32], five different RC-models with increasing complexity are formulated, trained and evaluated for each building type. In the simplest model, 1R1C, the thermodynamic properties are lumped together in only one capacitance and one resistance. The 2R2C model distinguishes between the fast dynamics of the indoor air and the inertia of the building envelope by introducing two capacitances. Besides, it uses two resistances for the heat transfer between the interior and the envelope as well as between the envelope and the ambient. The 3R2C model has an additional resistance for ventilation. The 4R3C model adds another capacitance for the heaters (radiators or underfloor heating depending on the building type). The 5R3C model extends the 4R3C model by a more detailed description of the radiative and convective heat transfers.

For grey-box modeling, the system equations of the individual RC-models are formulated as stochastic differential equations. RC-network representations as well as differential equations are available in Appendix C.

2.1.4 Parameter estimation

The parameters of the RC-models of each building type are estimated by the maximum likelihood method. A Kalman Filter is applied to calculate the likelihood function (see Ref. [28] on details). For the maximization of the likelihood function, the package "Continuous Time Stochastic Modeling" (CTSM) [55] in R [56] is used.

For each model parameter, upper and lower boundaries are defined in order to ensure that the estimated values are plausible from a physical point of view. Some of the parameter boundaries can be derived from the building typology (e.g. R_{ea} which is based on the transmission heat loss). For the boundaries of other parameters, standard physical quantities are used in addition to geometric information from the typology (e.g. C_i which is derived from the specific heat capacity of air and the building volume).

The RC-models are trained and validated by data simulated by TRNSYS as described in section 2.1.2. The indoor air temperature serves as observation data for parameter estimation. Heating power, solar radiation, ambient temperature and internal heat gains are taken as inputs. Different measures of solar radiation are tested in advance (see Figure B.1 on the course of different solar radiation data). It turns out that the total solar radiation on the southern vertical surface achieves the best goodness-of-fit. It has a course that is relatively proportional to the simulated solar gains. Thus, it is well suited for parameter estimation of a time-invariant system, as assumed here. Taking into account the total solar radiation on multiple surfaces, as done in study [34], does not improve the model performance. Common measures of solar radiation, like global horizontal irradiance (GHI), cannot outperform the total solar radiation on the southern vertical surface as input either.

The ideal composition of training data is evaluated beforehand for a subset of building types. First, the optimal length of training data is identified and found to be one month. Shorter datasets (e.g. two weeks) result in lower model quality, while longer datasets of two or more months cause overfitting. Second, different data periods are tested. It turns out that the optimal training dataset must have a high variability of the ambient temperature in order to produce a good model quality for the entire

heating period. Data from March (rather mild climate, see Appendix B), for example, is not suitable for reproducing test data in colder periods. Finally, data from January is identified as best suited for training. Data from the summer is not taken into account as it is irrelevant for the heating behavior and since cooling is not considered in this study.

For validation, two different datasets are used to test the generality of the models both for the full heating period (December, test data 1) and for the transition period containing longer phases without heating demand (October, test data 2).

2.1.5 Model evaluation

In order to evaluate the goodness-of-fit and applicability of the identified models, two indicators are assessed. The first indicator is model accuracy. It is measured by the RMSE, which indicates the difference between the indoor air temperature calculated by the RC-models and TRNSYS:

$$RMSE = 1/N * \sqrt{\sum_{t=1}^{N} (T_{i,RC,t} - T_{i,TRNSYS,t})^2} \quad \text{Eq. 3}$$

where N is the number of observations. For calculating RMSE, a distinction is made between simulated and predicted outputs of the RC-models (Figure 2). Simulated outputs rely only on input data of the test dataset and initial conditions. This form of computing model response is suitable for application in large-scale energy system models. Predicted outputs are calculated by additionally using output data of the test dataset in order to determine the model response at a specified time in the future, as it is often the case for model predictive control. Both measures are computed in this study to obtain a better comparability of the accuracy of the models with the literature.

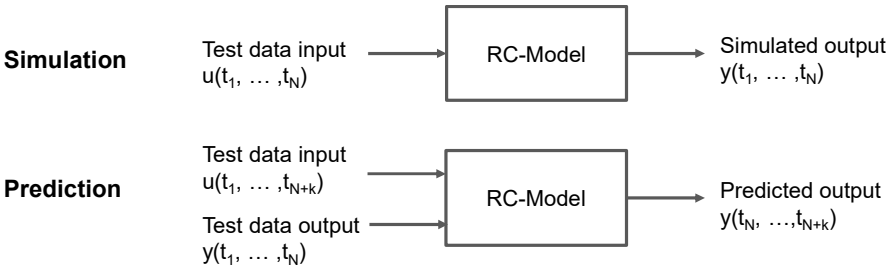


Figure 2: Principle of computing simulated and predicted outputs (adapted from [57])

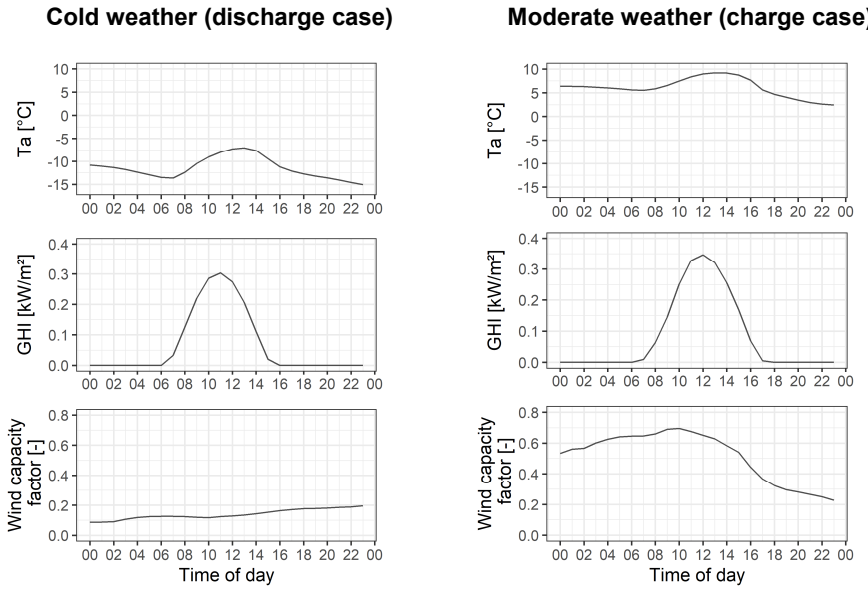
The second indicator is computational efficiency. To this end, the simulation duration of the RC-models and of TRNSYS is compared.

2.2 Calculation of the technical DR potential

For the quantification of heat pumps' technical potential for DR by passive storage in German SFH, the reduced-order models are applied for two predefined setups, which we consider to be the most relevant from an energy system perspective. Further setups are conceivable, but are beyond the scope of our study.

Like other studies [13,58], we distinguish between the DR potential for a discharge and a charge case. The discharge case refers to a DR intervention in which heat pumps are actively switched off, while the heat demand is met by discharging the passive storage. Vice versa, the charge case describes a DR intervention where heat pumps are actively switched on irrespective of the current heat demand by overheating the building thermal mass.

The DR potential of the structural thermal mass of buildings varies over time and is especially dependent on the ambient temperature [58]. We therefore consider a specific weather situation for each case. As a simplification, we assume that this weather situation is identical throughout Germany. For the discharge case, weather data of a very cold period in Germany is used (Figure 3, left) [59]. Such weather is of particular interest when assessing the DR potential of heat pumps for the reduction of backup capacity, because both the country-wide residual load and the heating load normally peak on the coldest days in Germany [60]. For the charge case, weather data of a rather mild day during the transition period is used (Figure 3, right). This situation is accompanied by rather high wind power generation, as can be seen from the corresponding wind capacity factor in Figure 3 [61]. The charge case serves to get an indication to what extent heat pumps can be actively controlled in order to integrate wind power generation.



352 Figure 3: Ambient temperature, GHI and wind capacity factor underlying the DR set-ups [59,61]

353 Following the approach of Hausladen et al. [13], the DR potential of individual building types is
354 determined by both shifted electrical load and duration of a DR intervention that multiplied results in an
355 energy value.

356 The shifted electrical load for each building type is set to the respective electrical heat pump power.
357 The latter is derived from the nominal boiler power at the design temperature of -14 °C (see section
358 2.1.2) as well as coefficients of performance (COP) of heat pumps. COP of air/water heat pumps and
359 brine/water heat pumps for different ambient conditions are taken and extrapolated from manufacturer
360 data [62–64]. They differ by the nominal flow temperature of the building types and are depicted in
361 Table 3. Building types with flow temperatures above 70 °C are not taken into account in the following
362 since they are only marginally relevant for heat pump application. For air/water heat pumps, the
363 electrical power is computed by dividing the nominal boiler power with the COP at an ambient
364 temperature (T_a) of -14 °C. As the manufacturer data imply, electrical heat pump power is
365 approximately constant also for warmer weather [62,64]. The heat output, instead, is calculated by the
366 COP values for the moderate weather (average T_a = 6°C). As a simplification, COPs are assumed to
367 be independent of weather conditions for brine/water heat pumps. The values in Table 3 refer to an
368 average brine inlet temperature of 0 °C.

Table 3: COPs used for the calculation of the electrical power of heat pumps

Flow temperature	COP air/water heat pump		COP brine/water heat pump
	T_a = -14 °C	T_a = 6 °C	
30-40 °C	2.4	4.5	4.8
41-50 °C	2.1	3.5	4.2
51-60 °C	1.7	2.9	3.1
61-70 °C	1.3	2.0	2.1

The second factor of DR potential, duration, measures the time until thermal comfort criteria are violated after a DR-induced shut-down or switch on of heat pumps. For the consideration of thermal comfort, the operative temperature (T_{op}) is used. It is defined as the mean value of the indoor air temperature (T_i) and of the radiation temperature of the surrounding surfaces (T_e). It is assumed that an acceptable thermal comfort is maintained as long as T_{op} is within a comfort band of 20 to 22 °C. For the discharge case, it is assumed that buildings are actively preheated to the upper comfort temperature before the DR intervention. For the charge case, buildings are assumed to be held at the lower comfort temperature before the DR intervention. The variation of the indoor temperature in the course of a DR intervention is thus set to 2 °C. For a sensitivity analysis, a reduction or increase of this variation to 1 °C and 3 °C is taken into account (Table 4).

Table 4: Initial and final values of the operative temperature during DR interventions

	Discharge case	Charge case
Initial T_{op}	22 °C	20 °C
Final T_{op}	20 °C ± 1 °C	22°C ± 1 °C

In a first step, the DR potential by passive storage is calculated for individual building types. The RC-models identified as optimal for each building type are used for the simulation of T_{op}. Afterwards, the potential is aggregated to the stock of German SFH according to their distribution (Table 2).

The aggregated DR potential is dependent on a) the market penetration of heat pumps and b) the insulation level of buildings. Consequently, two scenarios are defined. Presently, heat pumps account only for a small share of the building heat supply in Germany. Hence, future developments with a larger share of heat pumps are considered, as has widely been agreed upon [9]. The year 2040 is approximated in the scenarios. Regarding the market penetration of heat pumps, two pathways are defined. The pathway “50%_HP” assumes a market share of heat pumps of 50 %. As an upper limit, the pathway “Full_HP” implies a 100 % market penetration of heat pumps in order to estimate the

maximum potential of heat pumps for DR. It is assumed that the heat pump stock consists in equal proportion of air/water heat pumps and brine/water heat pumps. Two pathways are further defined for the second main parameter varied in the scenarios, insulation level. The moderate pathway “Conv_Retrofit” assumes that older buildings that were constructed before 2001 have already been retrofitted to Var2, according to an average renovation cycle of 40 years. Younger buildings are set to their original state (Var1). This translates into a distribution of 28 % Var1 buildings and 72 % Var2 buildings. The progressive pathway “Deep_Retrofit” is based on the assumption that all buildings are renovated to Var3 until 2040. New buildings (SFH L) are taken into account by extrapolating the average construction rate of SFH of the years 2016 to 2018 for both scenarios. Demolition of old buildings is not considered.

The calculation of the aggregated potential is based on the simplification that all heat pumps are controlled simultaneously for DR. This implies that the entire installed electrical capacity of heat pumps is available for load shifting. Since electrical power of heat pumps is assumed to be independent of weather conditions, shifted load is the same for both charge and the discharge case.

3 Results and discussion

In the following, the results for the model identification (section 3.1) and for the calculation of the DR potential (section 3.2) are presented and discussed separately.

3.1 Evaluation of identified reduced-order models

Results of the grey-box modeling are presented per defined evaluation indicators. The estimated parameters of the identified optimal models for each building type as well as corresponding RMSE can be found in the Appendix D. Note that individual parameters may have different physical meanings depending on the RC-model.

3.1.1 Model accuracy

Figure 4 summarizes the calculated RMSE for all building types differentiated by RC-models and test dataset. The values are based on the 24-h-ahead prediction as well as the simulation of the indoor air temperature over one month. As mentioned in section 2.1.5, predicted data are obtained by combining output data of the test dataset with the computation of the output of the RC-models 24 h in future. Simulated data, in contrast, rely only on initial conditions of TRNSYS and input data. RMSE are

reported separately for the building types without underfloor heating (SFH A to I) and with underfloor heating (SFH J to L) since these types differ with regard to optimal model complexity.

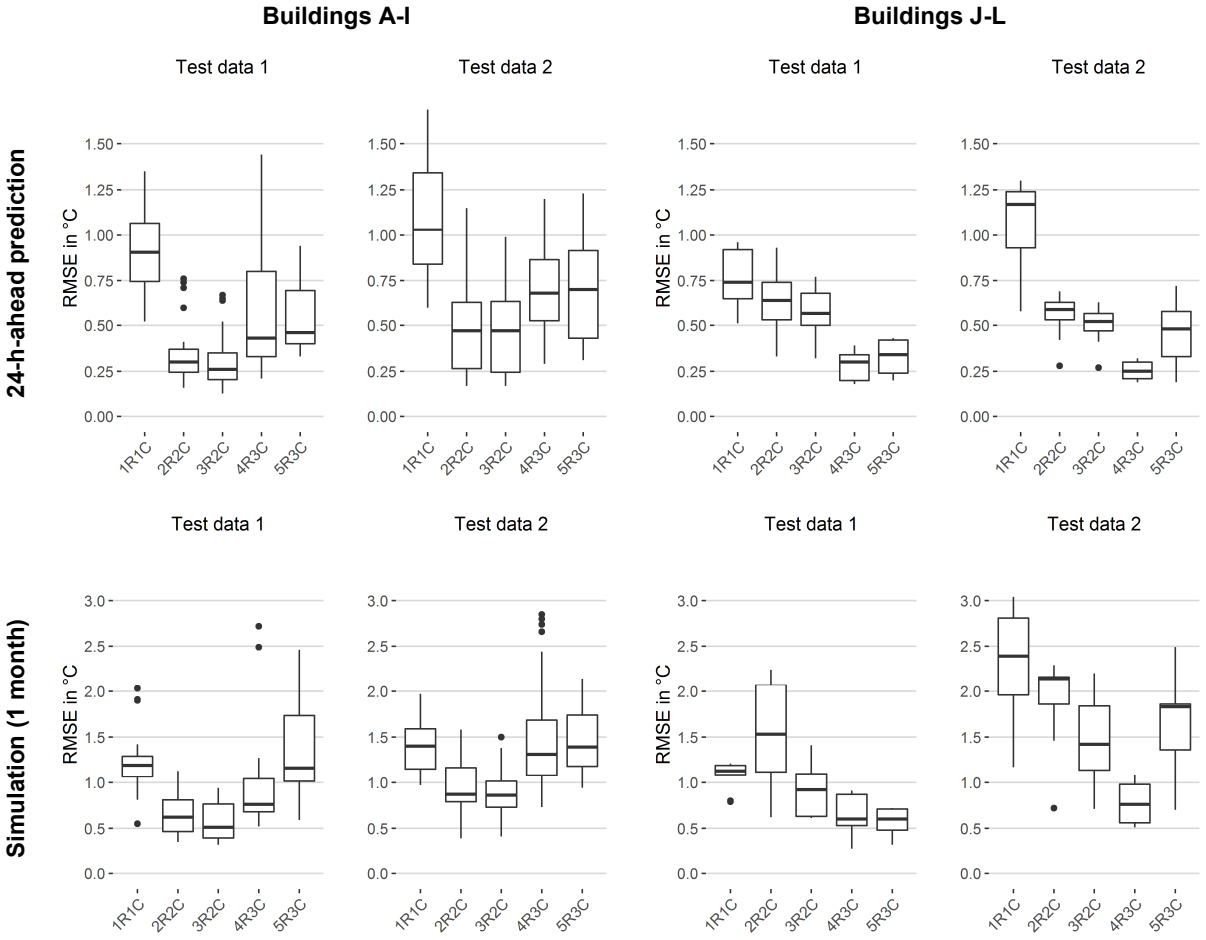


Figure 4: Range of RMSE values for all building types regarding 24-h-ahead prediction (upper plots) and simulation over one month (lower plots) of the indoor air temperature differentiated by RC-models and test data

In general, for all building types of a class (with / without underfloor heating) the same patterns can be observed regarding the optimal model complexity. For the building types without underfloor heating, the accuracy improves continuously from 1R1C to 3R2C, but decreases for the models with three capacitances. The optimal model for building types A to I is therefore the 3R2C model with a RMSE of on average 0.31 °C for the 24-h-ahead prediction and of 0.58 °C for the simulation over one month (test data 1).

For models with underfloor heating, however, the additional capacitance for heaters leads to a further improvement in model quality. The 4R3C model is more robust than the 5R3C model in terms of the test data and is therefore selected as the optimal model for the building types J to L. The mean RMSE is 0.28 °C for the 24-h-ahead prediction and 0.63 °C for the simulation over one month using test data

1. The identified optimal models are relatively robust in terms of the test dataset and thus of their applicability for the entire heating period. In general, however, the performance is better during the cold season (test data 1), which is advantageous due to its relevance for heating.

The accuracy of the identified models is comparable to that of previous studies (see section 1.3). Like Reynders et al. [38], we find that the type of heating system has a significant impact on optimal model complexity. However, while study [38] concludes that models with only one capacitance are already sufficient to capture the thermal response of buildings with underfloor heating, our study shows that at least three capacitances are needed for that case.

For illustration purposes, the simulated indoor air temperature of building type SFH F Var3 according to the estimated grey-box models 1R1C to 3R2C is compared to the reference TRNSYS data in Figure 5. The corresponding input data ambient temperature, heating power and solar radiation are shown in the lower three plots of Figure 5. Model 1R1C basically responds to changes in the inputs. However, it is particularly unsuitable to adequately reflect inert behavior (e.g. slow cooling during the night setback). The 2R2C model improves the performance significantly, stressing the importance of a second capacitance. The 3R2C model results in slight additional improvements.

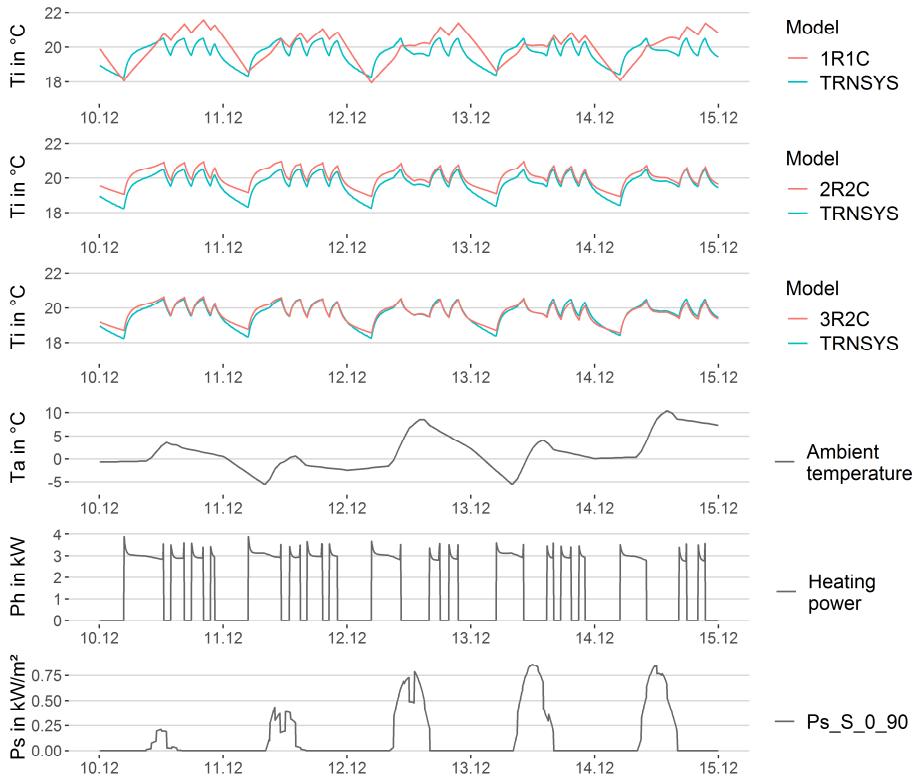


Figure 5: Simulation results for different RC-models compared to TRNSYS (upper three plots) and corresponding input data (lower three plots) for building SFH F Var3

3.1.2 Computational efficiency

Table 5 summarizes the average computation time for simulating the indoor air temperature of a building type for one year in six minutes resolution on a modern dual-core notebook (i7 processor) with 16 GB RAM. In comparison, simulations with TRNSYS lasted for on average 65 s for building types A to I with radiators and 80 s for building types J to L with underfloor heating on the same computer. Thus, an improvement of computational efficiency of a factor of about 250 is achieved for the respective most accurate RC-model. This acceleration is very relevant for energy system models that take about one minute to calculate power plant dispatch as well as stock exchange prices for just one year but usually simulate 30 to 50 years.

Table 5: Simulation time for RC-models for one year in six minutes resolution (average of all building types)

	1R1C	2R2C	3R2C	4R3C	5R3C
Average simulation time	0.11 s	0.24 s	0.25 s	0.33 s	0.34 s

3.1.3 General findings

By considering a wide variety of building types and RC-models, our study expands the knowledge on grey-box modeling of building thermodynamics. By comparing our findings to those of other relevant studies in this area (Table 1), the following general findings can be derived:

- Models with a minimum of two capacitances are required for a valid approximation of building thermodynamics for most building types.
- The type of heating system significantly affects optimal RC-model structure. However, the studies considered do not give a consistent indication as to whether buildings with underfloor heating require more or less complex models than buildings with radiator heating.
- A typology based grey-box modeling approach provides valid predictions of building thermal response compared to complex transient simulation software. A validation of such models by measured is currently limited due to a lack of data, but is highly desirable.

3.2 Technical DR potential by passive storage

Heat pumps' technical potential for DR by passive storage is first given for individual building types (section 3.2.1) and afterwards aggregated to the stock of German SFH (section 3.2.2).

3.2.1 DR potential of individual building types

Figure 6 summarizes the DR potential of all building types considered, separated by heat pump type. Both the shifted load and the DR potential in form of an electrical energy value are shown. The latter is the product of load and duration, depending on the case (discharge or charge potential). Error bars indicate sensitivities regarding a higher comfort band of 3 °C (upper limit of error bar) or lower comfort band of 1 °C (lower limit of error bar) compared to the reference comfort band of 2 °C.

As mentioned in section 2.2, the shifted loads are identical for the charge and the discharge case. They are higher for air/water heat pumps due to lower COP at design conditions compared to brine/water heat pumps. The shifted loads vary according to the construction period, insulation state and heated floor area. The highest shiftable loads are available in SFH G Var1 (11 kW_{el} for air/water heat pump), while only small loads of less than 2 kW_{el} can be shifted in most Var3 buildings.

Considering the discharge case, high loads are not necessarily reflected in high DR potentials. This is because poorly insulated buildings with high loads can delay further heat demand for only short durations due to high heat losses through the building envelope. Vice versa, low loads can be postponed for relatively long durations in well-insulated buildings. This is especially true for buildings with inert underfloor heating (SFH J to L). The resulting discharge potential ranges from 15 to 52 kWh_{el} per building for air/water heat pumps and from 8 to 32 kWh_{el} per building for brine/water heat pumps for the reference comfort band of 2 °C. An increase or decrease of the comfort band to 3 °C or 1 °C increases or decreases the discharge potential by half on average.

The charge potentials are generally lower than the discharge potentials. Especially buildings with radiator heating and high flow temperatures are heated up quite fast. This is particularly true when air/water heat pumps are applied, since their heat output rises with ambient temperatures[1]. In contrast, buildings with underfloor heating heat up slowly and thus provide a higher charge potential. Across both heat pump types, the charge potential varies between 3 and 29 kWh_{el} when assuming the reference comfort band of 2 °C. The charge potential is highly sensitive to changes in the comfort band for buildings with radiator heating: an increase to 3 °C doubles the potential for buildings with radiator heating, while a reduction to 1 °C lowers the potential by 60 % on average.

[1] With inverter heat pumps instead, which are gradually coming onto the market, the heat output is adapted to the current heat demand. For the charge potential, such heat pump types would offer a lower shifted load at higher durations.

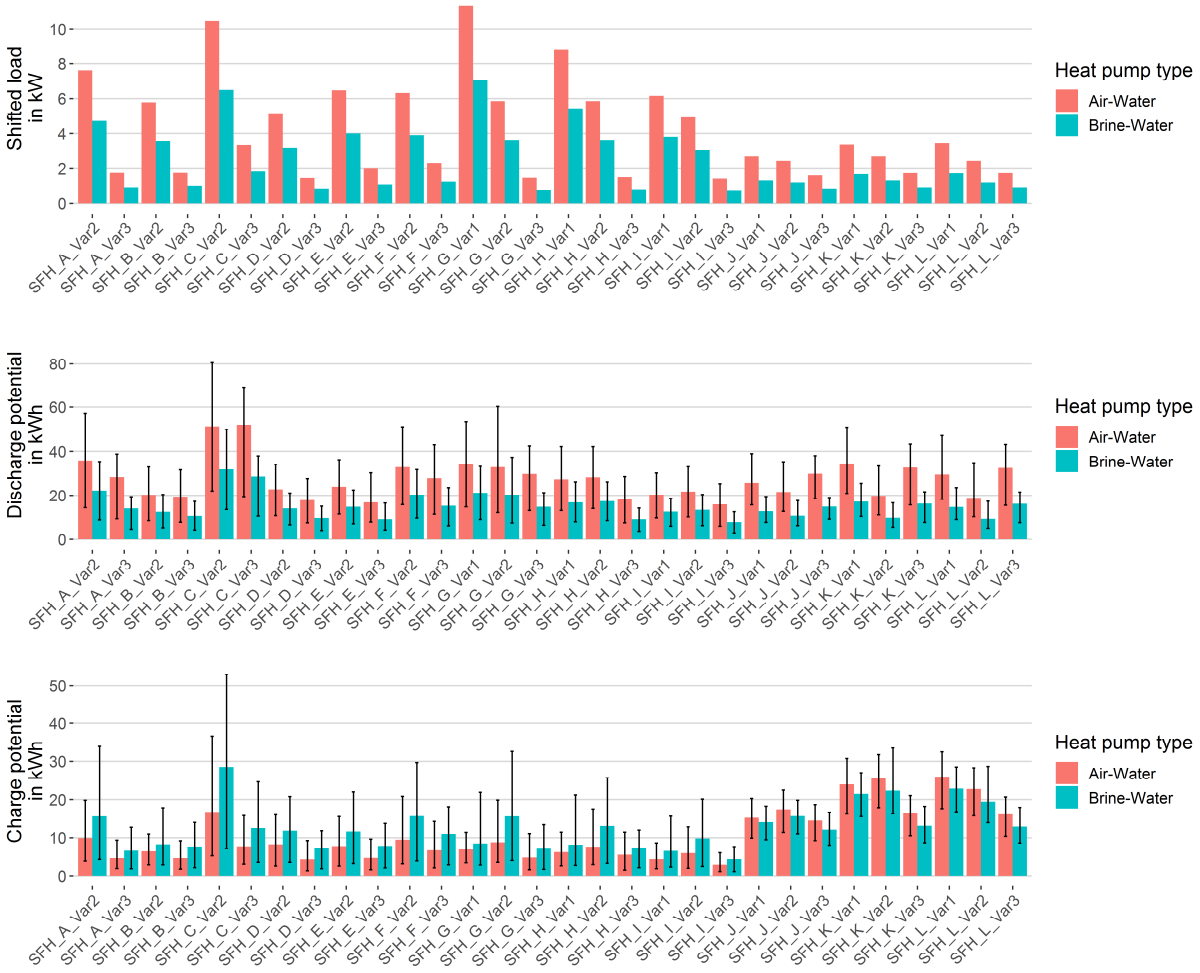


Figure 6: DR potential of individual building types, expressed as shifted electrical load (upper plot) as well as energy for the discharge case (middle plot) and the charge case (lower plot)

Taking the example of building type H, Figure 7 depicts the simulated discharging and charging behavior when employing an air/water heat pump. For the discharge case, it takes only about 3 h after the heat pump is powered off until the thermal comfort criterion is violated for the building in original condition (Var1). For the building with high insulation standard (Var3), the building cools down slowly over 12 h until it reaches the lower comfort temperature. Cooling is delayed by solar gains, which start around midday. Var1 is also the fastest to heat up after power on in the charge case (less than 1 h), while it takes more than 3 h for Var3 to reach the upper comfort temperature of 22 °C.

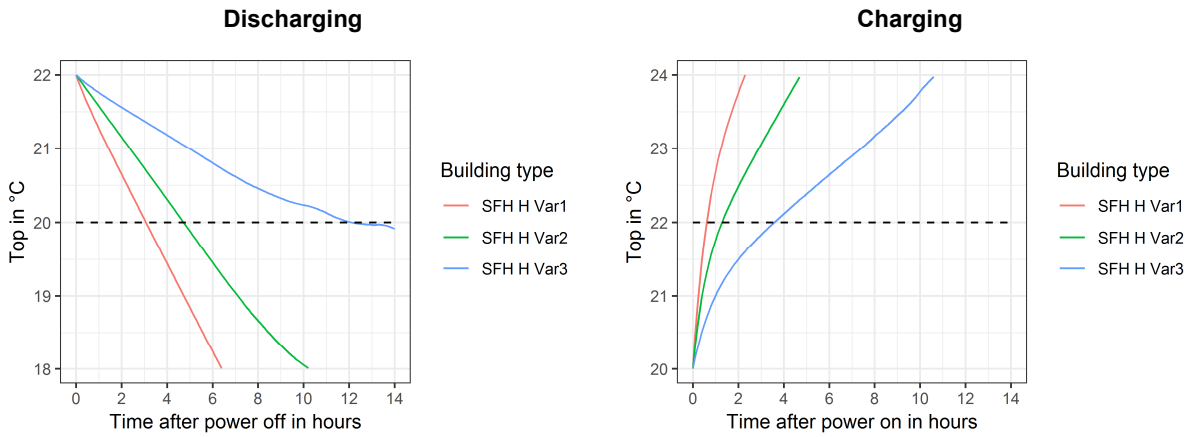


Figure 7: Simulation of the discharging and charging behavior of SFH H in three insulation conditions using the 3R2C model

3.2.2 DR potential of the stock of German SFH

The DR potential for the stock of German SFH is calculated by extrapolating the DR potentials for each individual building type. Results are shown in Figure 8. The maximum shifted load of heat pumps amounts to 57 GW_{el} when assuming the moderate insulation pathway (Conv_Retrofit) and full heat pump penetration. In the case of deep renovation, the shifted load is reduced to 18 GW_{el}. With only 50 % market penetration of heat pumps, the shifted load is also lowered by half.

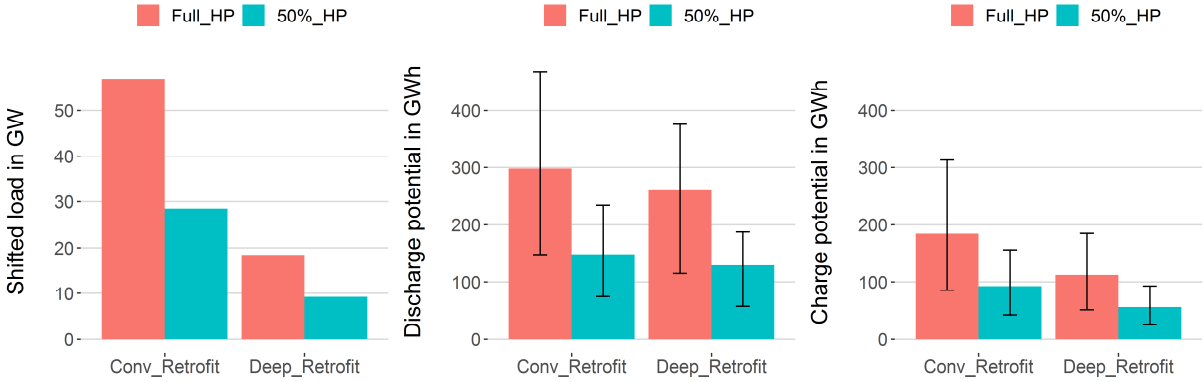


Figure 8: DR potential of the German stock of SFH for the four scenarios considered, expressed as shifted electrical load (left plot) and energy for the discharge case (middle plot) and the charge case (right plot)

Concerning the DR potential, a maximum of about 300 GWh_{el} can be “discharged” from the thermal mass of the building stock when taking into account full heat pump penetration and moderate insulation. Although durations are generally higher in deeply insulated buildings, the lower shiftable load causes the discharge potential to be only 260 GWh_{el} for full heat pump penetration in the Deep_Retrofit pathway. If only a 50 % heat pump penetration is assumed, the discharge potential

drops to 150 GWh_{el} (Conv_Retrofit) and 130 GWh_{el} (Deep_Retrofit) respectively. A reduction or increase of the comfort band to 1 °C or 3 °C reduces or increases the discharge potential by 50 % on average across all insulation and heat pump penetration pathways (see error bars).

For the charge case, the maximum potential adds up to 185 GWh_{el} (Conv_Retrofit, Full_HP). It reduces to 112 GWh_{el} for the Deep_Retrofit pathway. The 50%_HP pathway reduces the charge potential by half. The charge potential is quite sensitive to a change of the comfort band. A decrease to 1 °C reduces the charge potentials by about 55 % across all pathways. Changing the comfort band to 3 °C, instead, increases the charge potential by 70 %.

A comparison of the identified DR potentials to those of other studies is possible only to a limited extent, since corresponding calculations have hardly been presented for the future stock of German SFH to our knowledge. Hausladen et al. [13] estimate a maximum discharging potential of the passive storage of the existing stock of German residential and office buildings of around 76 GWh_{el} at a very cold winter day and a maximum charging potential of 113 GWh_{el} when taking into account moderate weather. However, a maximum duration of 2 h of a DR intervention is underlying their calculation of the electrical DR potential. Furthermore, the authors only differentiate between two classes of SFH (new and existing SFH) and do not take into account future insulation measures. For these reasons, the results are hardly comparable. Klobasa [65] calculates a DR potential from the area of residential cooling and electrical heating in Germany of 21 GW_{el} and 27 GWh_{el}. This is significantly lower than the findings from our study, since Klobasa only considers existing heating devices of the current building stock, with heat pumps having hardly been installed yet. Moreover, future well-insulated buildings with high duration potentials are not taken into account either.

The identified shiftable load of 9 to 57 GW_{el} can be considered as remarkably high when comparing it to the assumed backup capacities in long-term energy scenario studies. For example, Gerhardt et al. [49], who consider a share of 66 % of heat pumps for the German building sector in 2050, estimate that 27 GW of backup capacity based on natural gas is required for security of supply.

Due to the DR durations limited to a few hours to one day in buildings, passive storage through flexible operation of heat pumps in buildings is only suitable for short-term stabilization of the power system. Like most DR measures [18], its main function is thus to provide power rather than energy.

When interpreting the figures above, it should be kept in mind that the DR potential is estimated for two specific, but energy system analytically very relevant boundary conditions. In warmer periods than assumed for the discharge case, for example, the duration of a DR induced discharge can be increased due to reduced losses through the building shell. Vice versa, the charge potential would be smaller on cold days, since it takes longer to heat up buildings at low ambient temperatures.

Furthermore, it should be noted that the aggregated DR potential is strongly dependent on the underlying scenario for the development of the heating market. In this study, framework parameters such as heat pump penetration are in line with recent scenario studies [9]. Therefore, the identified aggregated DR potential should conform to transition pathways for the German energy system.

4 Conclusion

The present paper closes existing research gaps in the context of modeling DR with heat pumps in the German building stock. In the first part of the study, we present a set of reduced-order bottom-up models of the thermal response of typical buildings. The key novelty lies in the provision of computationally highly efficient and validated thermal response models which are representative for the entire stock of German SFH. The models enable fast simulation of the heat demand of buildings in a high temporal resolution as well as an evaluation of the DR potential of heat pumps by considering passive storage, by allowing for user preferences and by taking into account weather patterns.

Our investigation shows that linear reduced-order models based on grey-box modeling are very well suited for reflecting building thermodynamics. Using an electric analogy, buildings with radiator heating are best described by models with three resistances and two capacitances. If underfloor heating is employed, the optimal accuracy is achieved by more complex models with four resistances and three capacitances. Assuming a set point temperature of 20 °C in the heating period, the identified RC-models indicate an RMSE for the simulated indoor air temperature in the range of 0.3 to 0.9 °C compared to TRNSYS for a horizon of one month. At the same time, they are about 250 times faster than TRNSYS.

In the second part of this study, we provide an estimation of the technical DR potential of passive storage for the future stock of German SFH. We do so by applying our reduced-order models for a) a discharge case in very cold weather and b) a charge case for moderate ambient temperatures. We

show that the DR potential for both discharge and charge of passive storage is strongly dependent on the insulation standard and the heating system of the building. Projected to the total number of SFH in Germany, a total heat pump load of 9 to 57 GW_{el} can be shifted, depending on insulation measures and heat pump penetration. In very cold weather, this corresponds to 130 to 300 GWh_{el} that can be discharged from the passive storage. During milder days, 56 to 185 GWh_{el} can be charged into the structural thermal mass of buildings. Passive storage using heat pumps in buildings thus holds a remarkable potential for residual load shifting and renewable energy integration in a short-term perspective of several hours.

For an adequate system-wide quantification of the DR potential of passive storage, further dynamic factors (such as different weather conditions, interdependencies between charging and discharging and economic incentives for DR) need to be taken into account. These could be the subject of subsequent studies. The reduced-order models we provide are an important preliminary work for such system-wide investigations though, since they are suitable for integration into complex energy system models. Thus, these models allow system-level analyses on the integration of power and heat sectors, taking into account interactions between heterogeneous buildings and the energy markets.

This study has potential limitations. First of all, the parameters of the RC-models are estimated from the simulation model TRNSYS. In accordance to previous studies [33–36], no measurement data are applied to the development and validation of reduced-order models. This is simply due to a lack of measurement data for a complete and representative set of the German building stock. However, TRNSYS simulations have been validated in numerous studies (e.g. [66,67]) and therefore simulations constitute the best reference available. Second, this study is limited to SFH in Germany, which, however, make up two third of all buildings and are most relevant for heat pump application. Besides, the consideration of a wide variety of SFH types for grey-box modeling and calculation of the technical DR potential is an added value compared to many other studies from this field. Finally, the models are restricted to heating, not the cooling behavior of buildings. This is due to the fact that space heating currently accounts for about 70 % of final energy consumption of private households in Germany, while cooling is not very relevant (0.2 % of residential final energy consumption) [68]. The method presented here is, however, easily adaptable to the cooling behavior of buildings. This also applies for the transferability of the method to other building types within Germany (e.g. multistory buildings) or to buildings in other countries.

Acknowledgments

This work was supported by the German Federal Ministry of Education and Research within the Kopernikus project "Energy Transition Navigation System (ENavi)" (grant number 03SFK4D1). We gratefully acknowledge this support. We further thank the participants of the 7th International PhD Day of the AAEE Student Chapter, especially Lukas Kranzl, as well as Michael Nast for helpful discussions and valuable comments on an earlier version of this work. Finally, we thank the two anonymous reviewers whose insightful comments and suggestions helped improve and clarify this manuscript.

References

[1] J. Twidell, T. Weir, Renewable energy resources, Routledge, 2015. https://doi.org/https://doi.org/10.4324/9781315766416.

[2] K. Schaber, F. Steinke, T. Hamacher, Transmission grid extensions for the integration of variable renewable energies in Europe: Who benefits where?, EnergyPolicy. 43 (2012) 123–135. https://doi.org/http://dx.doi.org/10.1016/j.enpol.2011.12.040.

[3] S.O. Amrouche, D. Rekioua, T. Rekioua, S. Bacha, Overview of energy storage in renewable energy systems, InternationalJournal Hydrogen Energy. 41 (2016) 20914–20927. https://doi.org/https://doi.org/10.1016/j.ijhydene.2016.06.243.

[4] M. Kubik, P.J. Coker, J.F. Barlow, Increasing thermal plant flexibility in a high renewables power system, AppliedEnergy. 154 (2015) 102–111. https://doi.org/https://doi.org/10.1016/j.apenergy.2015.04.063.

[5] P. Siano, Demand response and smart grids—A survey, Renewable sustainable energy reviews. 30 (2014) 461–478. https://doi.org/https://doi.org/10.1016/j.rser.2013.10.022.

[6] A. Bloess, W.-P. Schill, A. Zerrahn, Power-to-heat for renewable energy integration: A review of technologies, modeling approaches, and flexibility potentials, AppliedEnergy. 212 (2018) 1611–1626. https://doi.org/https://doi.org/10.1016/j.apenergy.2017.12.073.

[7] K. Hedegaard, M. Münster, Influence of individual heat pumps on wind power integration: Energy system investments and operation, EnergyConversion Management. 75 (2013) 673–684. https://doi.org/http://dx.doi.org/10.1016/j.enconman.2013.08.015.

[8] M.Z. Jacobson, M.A. Delucchi, Z.A.F. Bauer, S.C. Goodman, W.E. Chapman, M.A. Cameron, C. Bozonnat, L. Chobadi, H.A. Clonts, P. Enevoldsen, J.R. Erwin, S.N. Fobi, O.K. Goldstrom, E.M. Hennessy, J. Liu, J. Lo, C.B. Meyer, S.B. Morris, K.R. Moy, P.L. O'Neill, I. Petkov, S. Redfern, R. Schucker, M.A. Sontag, J. Wang, E. Weiner, A.S. Yachanin, 100% Clean and Renewable Wind, Water, and Sunlight All-Sector Energy Roadmaps for 139 Countries in the World, Joule. 1 (2017) 108–121. https://doi.org/doi: 10.1016/j.joule.2017.07.005.

[9] O. Ruhnau, S. Bannik, S. Otten, A. Praktiknjo, M. Robinius, Direct or indirect electrification? A review of heat generation and road transport decarbonisation scenarios for Germany 2050, Energy. 166 (2019) 989–999. https://doi.org/https://doi.org/10.1016/j.energy.2018.10.114.

[10] G. Papaefthymiou, B. Hasche, C. Nabe, Potential of Heat Pumps for Demand Side Management and Wind Power Integration in the German Electricity Market, IEEETransactions Sustainable Energy. 3 (2012) 636–642. https://doi.org/10.1109/TSTE.2012.2202132.

[11] B. Pfluger, B. Tersteegen, B. Franke, Langfristszenarien für die Transformation des Energiesystems in Deutschland, Fraunhofer ISI, Consentec GmbH, ifeu, Bundesministerium für Wirtschaft und Energie, 2017. https://www.bmwi.de/Redaktion/DE/Artikel/Energie/langfrist-und-klimaszenarien.html.

[12] O. Ruhnau, L. Hirth, A. Praktiknjo, Heating with wind:Economics of heat pumps and variable renewables, Econstor. (2019). http://hdl.handle.net/10419/206688.

[13] G. Hausladen, T. Auer, J. Schneegans, K. Klimke, H. Riemer, B. Trojer, L. Qian, M. de Borja Torrejon, Lastverhalten von Gebäuden unter Berücksichtigung unterschiedlicher Bauweisen und technischer Systeme. Speicher-und Lastmanagementpotenziale in Gebäuden, Lehrstuhl für Gebäudetechnologie und klimagerechtes Bauen, 2014.

[14] J. Le Dréau, P. Heiselberg, Energy flexibility of residential buildings using short term heat storage in the thermal mass, Energy. 111 (2016) 991–1002. https://doi.org/https://doi.org/10.1016/j.energy.2016.05.076.
[15] J. Hong, N.J. Kelly, I. Richardson, M. Thomson, Assessing heat pumps as flexible load, Proceedings InstitutionMechanicalEngineers,PartAJournal PowerEnergy. 227 (2013) 30–42. https://doi.org/https://doi.org/10.1177/0957650912454830.
[16] A. Palzer, H.-M. Henning, A comprehensive model for the German electricity and heat sector in a future energy system with a dominant contribution from renewable energy technologies-Part II: Results, Renewable Sustainable Energy Reviews. 30 (2014) 1019–1034. https://doi.org/http://dx.doi.org/10.1016/j.rser.2013.11.032.
[17] D. Fehrenbach, E. Merkel, R. McKenna, U. Karl, W. Fichtner, On the economic potential for electric load management in the German residential heating sector - An optimising energy system model approach, Energy. 71 (2014) 263–276. https://doi.org/https://doi.org/10.1016/j.energy.2014.04.061.
[18] H.C. Gils, Economic potential for future demand response in Germany–Modeling approach and case study, AppliedEnergy. 162 (2016) 401–415. https://doi.org/https://doi.org/10.1016/j.apenergy.2015.10.083.
[19] A. Arteconi, N.J. Hewitt, F. Polonara, Domestic demand-side management (DSM): Role of heat pumps and thermal energy storage (TES) systems, AppliedThermalEngineering. 51 (2013) 155–165. https://doi.org/http://dx.doi.org/10.1016/j.applthermaleng.2012.09.023.
[20] L. Kotzur, Future grid load of the residential building sector, RWTH Aachen University, 2018.
[21] R.E. Hedegaard, S. Petersen, Evaluation of grey-box model parameter estimates intended for thermal characterization of buildings, EnergyProcedia. 132 (2017) 982–987. https://doi.org/https://doi.org/10.1016/j.egypro.2017.09.692.
[22] R. Bruno, G. Pizzuti, N. Arcuri, The prediction of thermal loads in building by means of the EN ISO 13790 dynamic model: A comparison with TRNSYS, EnergyProcedia. 101 (2016) 192–199. https://doi.org/https://doi.org/10.1016/j.egypro.2016.11.025.
[23] K. Hedegaard, O. Balyk, Energy system investment model incorporating heat pumps with thermal storage in buildings and buffer tanks, Energy. 63 (2013) 356–365. https://doi.org/https://doi.org/10.1016/j.energy.2013.09.061.
[24] B. Baeten, F. Rogiers, L. Helsen, Reduction of heat pump induced peak electricity use and required generation capacity through thermal energy storage and demand response, AppliedEnergy. 195 (2017) 184–195. https://doi.org/dx.doi.org/10.1016/j.apenergy.2017.03.055.
[25] A. Arteconi, D. Patteeuw, K. Bruninx, E. Delarue, W. D'haeseleer, L. Helsen, Active demand response with electric heating systems: Impact of market penetration, AppliedEnergy. 177 (2016) 636–648. https://doi.org/https://doi.org/10.1016/j.apenergy.2016.05.146.
[26] D. Patteeuw, G. Reynders, K. Bruninx, C. Protopapadaki, E. Delarue, W. D'haeseleer, D. Saelens, L. Helsen, CO2-abatement cost of residential heat pumps with active demand response: demand-and supply-side effects, AppliedEnergy. 156 (2015) 490–501. https://doi.org/https://doi.org/10.1016/j.apenergy.2015.07.038.
[27] D. Patteeuw, K. Bruninx, A. Arteconi, E. Delarue, W. D'haeseleer, L. Helsen, Integrated modeling of active demand response with electric heating systems coupled to thermal energy storage systems, AppliedEnergy. 151 (2015) 306–319. https://doi.org/https://doi.org/10.1016/j.apenergy.2015.04.014.
[28] N.R. Kristensen, H. Madsen, S.B. Jørgensen, Parameter estimation in stochastic grey-box models, Automatica. 40 (2004) 225–237. https://doi.org/https://doi.org/10.1016/j.automatica.2003.10.001.
[29] V. Harish, A. Kumar, A review on modeling and simulation of building energy systems, Renewable Sustainable Energy Reviews. 56 (2016) 1272–1292. https://doi.org/https://doi.org/10.1016/j.rser.2015.12.040.
[30] A. Bagheri, V. Feldheim, C.S. Ioakimidis, On the evolution and application of the thermal network method for energy assessments in buildings, Energies. 11 (2018) 890. https://doi.org/https://doi.org/10.3390/en11040890.
[31] D. Coley, J. Penman, Second order system identification in the thermal response of real buildings. Paper II: recursive formulation for on-line building energy management and control, Building Environment. 27 (1992) 269–277. https://doi.org/https://doi.org/10.1016/0360-1323(92)90028-N.
[32] P. Bacher, H. Madsen, Identifying suitable models for the heat dynamics of buildings, Energy Buildings. 43 (2011) 1511–1522. https://doi.org/https://doi.org/10.1016/j.enbuild.2011.02.005.

[33] I. Hazyuk, C. Ghiaus, D. Penhouet, Optimal temperature control of intermittently heated buildings using Model Predictive Control: Part I–Building modeling, Building Environment. 51 (2012) 379–387. https://doi.org/https://doi.org/10.1016/j.buildenv.2011.11.009.
[34] G. Reynders, J. Diriken, D. Saelens, Quality of grey-box models and identified parameters as function of the accuracy of input and observation signals, Energy Buildings. 82 (2014) 263–274. https://doi.org/https://doi.org/10.1016/j.enbuild.2014.07.025.
[35] G. Reynders, J. Diriken, D. Saelens, Bottom-up modeling of the Belgian residential building stock: influence of model complexity, SSB. 2014 (2014) 1–19.
[36] T. Berthou, P. Stabat, R. Salvazet, D. Marchio, Development and validation of a gray box model to predict thermal behavior of occupied office buildings, Energy Buildings. 74 (2014) 91–100. https://doi.org/https://doi.org/10.1016/j.enbuild.2014.01.038.
[37] S.F. Fux, A. Ashouri, M.J. Benz, L. Guzzella, EKF based self-adaptive thermal model for a passive house, Energy Buildings. 68 (2014) 811–817. https://doi.org/https://doi.org/10.1016/j.enbuild.2012.06.016.
[38] G. Reynders, J. Diriken, D. Saelens, Impact of the heat emission system on the identification of grey-box models for residential buildings, EnergyProcedia. 78 (2015) 3300–3305. https://doi.org/https://doi.org/10.1016/j.egypro.2015.11.740.
[39] V. Dimitriou, Lumped parameter thermal modelling for UK domestic buildings based on measured operational data, Loughborough University, 2016.
[40] H. Harb, N. Boyanov, L. Hernandez, R. Streblow, D. Müller, Development and validation of grey-box models for forecasting the thermal response of occupied buildings, Energy Buildings. 117 (2016) 199–207. https://doi.org/https://doi.org/10.1016/j.enbuild.2016.02.021.
[41] A. Fonti, G. Comodi, S. Pizzuti, A. Arteconi, L. Helsen, Low order grey-box models for short-term thermal behavior prediction in buildings, EnergyProcedia. 105 (2017) 2107–2112. https://doi.org/https://doi.org/10.1016/j.egypro.2017.03.592.
[42] M. Massano, E. Macii, E. Patti, A. Acquaviva, L. Bottaccioli, A Grey-box Model Based on Unscented Kalman Filter to Estimate Thermal Dynamics in Buildings, in: 2019IEEEInternationalConference EnvironmentElectricalEngineering 2019 IEEE IndustrialCommercialPowerSystemsEurope(EEEIC/I&CPSEurope), IEEE, 2019: pp. 1–6. https://doi.org/10.1109/EEEIC.2019.8783974.
[43] I. Ballarini, S.P. Corgnati, V. Corrado, Use of reference buildings to assess the energy saving potentials of the residential building stock: The experience of TABULA project, EnergyPolicy. 68 (2014) 273–284. https://doi.org/https://doi.org/10.1016/j.enpol.2014.01.027.
[44] W. Cyx, N. Renders, M. Van Holm, S. Verbeke, IEE TABULA-typology approach for building stock energy assessment, 2011.
[45] T. Loga, B. Stein, N. Diefenbach, R. Born, Deutsche Wohngebäudetypologie. Beispielhafte Maßnahmen zur Verbesserung der Energieeffizienz von typischen Wohngebäuden, Institut Wohnen und Umwelt, 2015.
[46] Eurostat, Final energy consumption in households by type of fuel, (2020). https://ec.europa.eu/eurostat/databrowser/view/ten00125/default/table?lang=en.
[47] H. Lund, B. Möller, B.V. Mathiesen, A. Dyrelund, The role of district heating in future renewable energy systems, Energy. 35 (2010) 1381–1390. https://doi.org/http://dx.doi.org/10.1016/j.energy.2009.11.023.
[48] Statistische Ämter des Bundes und der Länder, Zensus 2011, Gebäude- und Wohnungsbestand in Deutschland, Endgültige Ergebnisse, 2015. www.statistikportal.de.
[49] N. Gerhardt, I. Ganal, M. Jentsch, J. Rodriguez, K. Stroh, E.K. Buchmann, Entwicklung der Gebäudewärme und Rückkopplung mit dem Energiesystem in -95% THG-Klimazielszenarnien, Fraunhofer-Institut für Energiewirtschaft und Energiesystemtechnik (Fraunhofer IEE), 2019.
[50] Statistisches Bundesamt (DESTATIS, Bauen und Wohnen, Baugemehmigungen / Baufertigstellungen u.a. nach Gebäudeart, (2019).
[51] Sa. Klein, A. Beckman, W. Mitchell, A. Duffie, TRNSYS 17-A TRansient SYstems Simulation program, SolarEnergyLaboratory,University Wisconsin, Madison. (2011).
[52] C. Protopapadaki, G. Reynders, D. Saelens, Bottom-up modelling of the Belgian residential building stock: impact of building stock descriptions, in: Proceedings 9th International ConferenceSystemSimulation Buildings-SSB2014, Belgium, 2014.
[53] J. Lam, M. Hiller, Schwierigkeiten bei der Verwendung der TRY Daten 2011 für Deutschland in der thermischen Simulation, in: Proceedings5thGermanAustrianIBPSAConferenceBauSIM2014,Aachen, 2014: pp. 395–401.
[54] Meteotest, Meteonorm v5.0 Global Meteorological Database for Solar Energy and Applied Climatology, (2003).

[55] R. Juhl, J.K. Møller, H. Madsen, ctsmr-Continuous Time Stochastic Modeling in R, arXivpreprintarXiv:1606.00242. (2016).
[56] R.C. Team, R: A Language and Environment for Statistical Computing, R Foundation for Statistical Computing, Vienna, Austria, 2018. https://www.R-project.org/.
[57] MathWorks, Simulate and Predict Identified Model Output, (2020). https://de.mathworks.com/help/ident/ug/definition-simulation-and-prediction.html.
[58] G. Reynders, J. Diriken, D. Saelens, Generic characterization method for energy flexibility: Applied to structural thermal storage in residential buildings, AppliedEnergy. 198 (2017) 192–202. https://doi.org/https://doi.org/10.1016/j.apenergy.2017.04.061.
[59] Open Power System Data, Data Platfrom Weather Data, (2020). https://doi.org/https://doi.org/10.25832/weather_data/2019-04-09.
[60] K. Klein, S. Killinger, D. Fischer, C. Streuling, J. Salom, E. Cubi, Comparison of the future residual load in fifteen countries and requirements to grid-supportive building operation, in: Proceedings 11th EuroSun Conference, Palma, Spain, 2016: pp. 11–14.
[61] Open Power System Data, Data Platfrom Time series, (2020). https://doi.org/https://doi.org/10.25832/time_series/2019-06-05.
[62] Dimplex, Geräteinformation Wärmepumpe, (2020). http://www.dimplex.de/fileadmin/dimplex/downloads/projektierungshandbuecher/de/496-geraeteinformationen-wp-08-2012.pdf.
[63] Daikin, Katalog 2019-2020 Heizen, (2020). https://www.daikin.at/content/dam/DACE-AT/document-library/catalogues/heat/DAIKIN%20Katalog%20HEIZUNG%202019.pdf.
[64] Effiziento, Projektierungshandbuch Haustechnikzentrale, Luft/Wasser Wärmepumpe, Lüftungsgerät / Wärmespeicher, (2020). https://www.effiziento.de/fileadmin/Download/PH_HTZ_LI_LG_PS_Zubehoer.pdf.
[65] M. Klobasa, Analysis of demand response and wind integration in Germany's electricity market, RenewablePowerGeneration,IET. 4 (2010) 55–63. https://doi.org/10.1049/iet-rpg.2008.0086.
[66] K. Lomas, H. Eppel, C. Martin, D. Bloomfield, Empirical validation of building energy simulation programs, Energy buildings. 26 (1997) 253–275. https://doi.org/https://doi.org/10.1016/S0378-7788(97)00007-8.
[67] J. Aschaber, M. Hiller, R. Weber, others, TRNSYS17: New features of the multizone building model, in: 11thInternationalBuildingPerformanceSimulationAssociationConference, Citeseer, 2009.
[68] BMWi, Zahlen und Fakten Energiedaten, Nationale und Internationale Entwicklung, Stand Januar 2019, (2019). https://www.bmwi.de/Redaktion/DE/Artikel/Energie/energiedaten-gesamtausgabe.html.

Appendix A: Thermal characteristics of building types

Table A.1: Construction, U-values and specific heat demand of building types according to the German building typology [45]. Note that own assumptions are made with regard to floor covering

Building code	External walls		Floor		Roof		Windows	Heat demand in kWh/(m²,K)
	Construction	U-Value in W/(m²,K)	Construction	U-Value in W/(m²,K)	Construction	U-Value in W/(m²,K)	U-Value in W/(m²,K)	
SFH A	Half-timbered	Var1: 2.00 Var2: 0.35 Var3: 0.14	Stone floor on soil	Var1: 2.90 Var2: 0.49 Var3: 0.27	Wooden rafters, empty compartment	Var1: 2.60 Var2: 0.41 Var3: 0.14	Var1: 2.80 Var2: 1.60 Var3: 0.80	Var1: 323.7 Var2: 108.5 Var3: 29.9
SFH B	Solid brickwork	Var1: 1.70 Var2: 0.25 Var3: 0.13	Wooden beams	Var1: 1.20 Var2: 0.32 Var3: 0.23	Wooden rafters, clay	Var1: 1.30 Var2: 0.41 Var3: 0.14	Var1: 2.80 Var2: 1.60 Var3: 0.80	Var1: 308.6 Var2: 112.7 Var3: 39.6
SFH C	Solid brickwork	Var1: 1.70 Var2: 0.25 Var3: 0.13	Steel girder with wooden floor	Var1: 1.00 Var2: 0.30 Var3: 0.23	Wooden rafters, empty compartment	Var1: 1.40 Var2: 0.41 Var3: 0.14	Var1: 2.80 Var2: 1.30 Var3: 0.80	Var1: 250.2 Var2: 95.6 Var3: 32.0
SFH D	Bivalve masonry	Var1: 1.40 Var2: 0.40 Var3: 0.13	Concrete with wooden floor boards	Var1: 1.00 Var2: 0.31 Var3: 0.23	Wooden rafters, bricked compartment	Var1: 1.40 Var2: 0.41 Var3: 0.14	Var1: 2.80 Var2: 1.30 Var3: 0.80	Var1: 312.5 Var2: 136.6 Var3: 44.4
SFH E	Hollow brick masonry	Var1: 1.20 Var2: 0.23 Var3: 0.13	Concrete, parquet flooring	Var1: 1.60 Var2: 0.34 Var3: 0.25	Wooden rafters	Var1: 0.80 Var2: 0.41 Var3: 0.14	Var1: 2.80 Var2: 1.30 Var3: 0.80	Var1: 303.2 Var2: 146.3 Var3: 54.3
SFH F	Hollow brick masonry	Var1: 1.00 Var2: 0.22 Var3: 0.13	Concrete, tiles	Var1: 1.00 Var2: 0.30 Var3: 0.23	Flat roof made of reinforced concrete	Var1: 0.50 Var2: 0.18 Var3: 0.09	Var1: 2.80 Var2: 1.30 Var3: 0.80	Var1: 223.6 Var2: 104.8 Var3: 41.2
SFH G	Light perforated bricks masonry	Var1: 0.80 Var2: 0.21 Var3: 0.12	Concrete, tiles	Var1: 0.80 Var2: 0.28 Var3: 0.21	Wooden rafters	Var1: 0.50 Var2: 0.41 Var3: 0.14	Var1: 4.30 Var2: 1.30 Var3: 0.80	Var1: 149.3 Var2: 84.0 Var3: 25.9
SFH H	Aerated concrete masonry	Var1: 0.50 Var2: 0.18 Var3: 0.11	Concrete, tiles	Var1: 0.60 Var2: 0.25 Var3: 0.20	Wooden rafters	Var1: 0.40 Var2: 0.41 Var3: 0.14	Var1: 3.20 Var2: 1.30 Var3: 0.80	Var1: 173.7 Var2: 110.5 Var3: 39.7
SFH I	Monolithic masonry	Var1: 0.30 Var2: 0.15 Var3: 0.14	Concrete, parquet flooring	Var1: 0.45 Var2: 0.22 Var3: 0.18	Wooden rafters	Var1: 0.35 Var2: 0.41 Var3: 0.14	Var1: 1.90 Var2: 1.30 Var3: 0.80	Var1: 134.9 Var2: 109.6 Var3: 41.1
SFH J	Monolithic masonry	Var1: 0.30 Var2: 0.15	Concrete, tiles	Var1: 0.30 Var2: 0.18	Wooden rafters	Var1: 0.25 Var2: 0.41	Var1: 1.40 Var2: 1.30	Var1: 82.0 Var2: 78.8

		Var3:	0.14		Var3:	0.18		Var3:	0.14	Var3:	0.80	Var3:	37.4
SFH K	Sand-lime brickwork	Var1:	0.23	Concrete,	Var1:	0.30	Wooden rafters	Var1:	0.20	Var1:	1.30	Var1:	94.3
		Var2:	0.20	parquet flooring	Var2:	0.24		Var2:	0.16	Var2:	1.30	Var2:	81.7
		Var3:	0.12		Var3:	0.12		Var3:	0.10	Var3:	0.70	Var3:	25.5
SFH L	Sand-lime brickwork	Var1:	0.30	Concrete,	Var1:	0.30	Wooden rafters	Var1:	0.26	Var1:	1.10	Var1:	102.3
		Var2:	0.15	parquet flooring	Var2:	0.15		Var2:	0.13	Var2:	1.10	Var2:	73.9
		Var3:	0.12		Var3:	0.12		Var3:	0.10	Var3:	0.70	Var3:	25.5

828 Table A.2: Specification of the heating system of building types (own assumptions and calculations)

Building type	Nominal boiler power		Type of heaters	Nominal flow /return temperature		Hysteresis	
SFH A	Var1:	30.8 kW	Radiators	Var1:	80 / 60 °C	Var1:	2 °C
	Var2:	9.9 kW		Var2:	70 / 55 °C	Var2:	1 °C
	Var3:	3.7 kW		Var3:	50 / 40 °C	Var3:	1 °C
SFH B	Var1:	19.1 kW	Radiators	Var1:	75 / 60 °C	Var1:	2 °C
	Var2:	7.5 kW		Var2:	70 / 55 °C	Var2:	1 °C
	Var3:	3.0 kW		Var3:	55 / 45 °C	Var3:	1 °C
SFH C	Var1:	32.4 kW	Radiators	Var1:	80 / 60 °C	Var1:	2 °C
	Var2:	13.6 kW		Var2:	70 / 55 °C	Var2:	1 °C
	Var3:	5.7 kW		Var3:	55 / 45 °C	Var3:	1 °C
SFH D	Var1:	15.9 kW	Radiators	Var1:	75 / 60 °C	Var1:	2 °C
	Var2:	6.7 kW		Var2:	70 / 55 °C	Var2:	1 °C
	Var3:	2.5 kW		Var3:	55 / 45 °C	Var3:	1 °C
SFH E	Var1:	17.8 kW	Radiators	Var1:	75 / 60 °C	Var1:	2 °C
	Var2:	8.4 kW		Var2:	70 / 55 °C	Var2:	1 °C
	Var3:	3.4 kW		Var3:	55 / 45 °C	Var3:	1 °C
SFH F	Var1:	17.2 kW	Radiators	Var1:	75 / 60 °C	Var1:	2 °C
	Var2:	8.2 kW		Var2:	70 / 55 °C	Var2:	1 °C
	Var3:	3.9 kW		Var3:	55 / 45 °C	Var3:	1 °C
SFH G	Var1:	14.8 kW	Radiators	Var1:	70 / 55 °C	Var1:	2 °C
	Var2:	7.6 kW		Var2:	65 / 50 °C	Var2:	1 °C
	Var3:	3.1 kW		Var3:	50 / 40 °C	Var3:	1 °C
SFH H	Var1:	11.4 kW	Radiators	Var1:	65 / 50 °C	Var1:	2 °C
	Var2:	7.6 kW		Var2:	65 / 50 °C	Var2:	1 °C
	Var3:	3.2 kW		Var3:	50 / 40 °C	Var3:	1 °C
SFH I	Var1:	8.0 kW	Radiators	Var1:	65 / 50 °C	Var1:	2 °C
	Var2:	6.4 kW		Var2:	65 / 50 °C	Var2:	1 °C
	Var3:	3.0 kW		Var3:	50 / 40 °C	Var3:	1 °C
SFH J	Var1:	6.4 kW	Underfloor heating	Var1:	40 / 30 °C	Var1:	1 °C
	Var2:	5.8 kW		Var2:	35 / 28 °C	Var2:	1 °C
	Var3:	3.9 kW		Var3:	33 / 27 °C	Var3:	1 °C
SFH K	Var1:	8.1 kW	Underfloor heating	Var1:	40 / 30 °C	Var1:	1 °C
	Var2:	6.4 kW		Var2:	35 / 28 °C	Var2:	1 °C
	Var3:	4.2 kW		Var3:	30 / 25 °C	Var3:	1 °C
SFH L	Var1:	8.3 kW	Underfloor heating	Var1:	40 / 30 °C	Var1:	1 °C
	Var2:	5.8 kW		Var2:	35 / 28 °C	Var2:	1 °C
	Var3:	4.2 kW		Var3:	30 / 25 °C	Var3:	1 °C

829

Appendix B: Weather data used for grey-box modeling

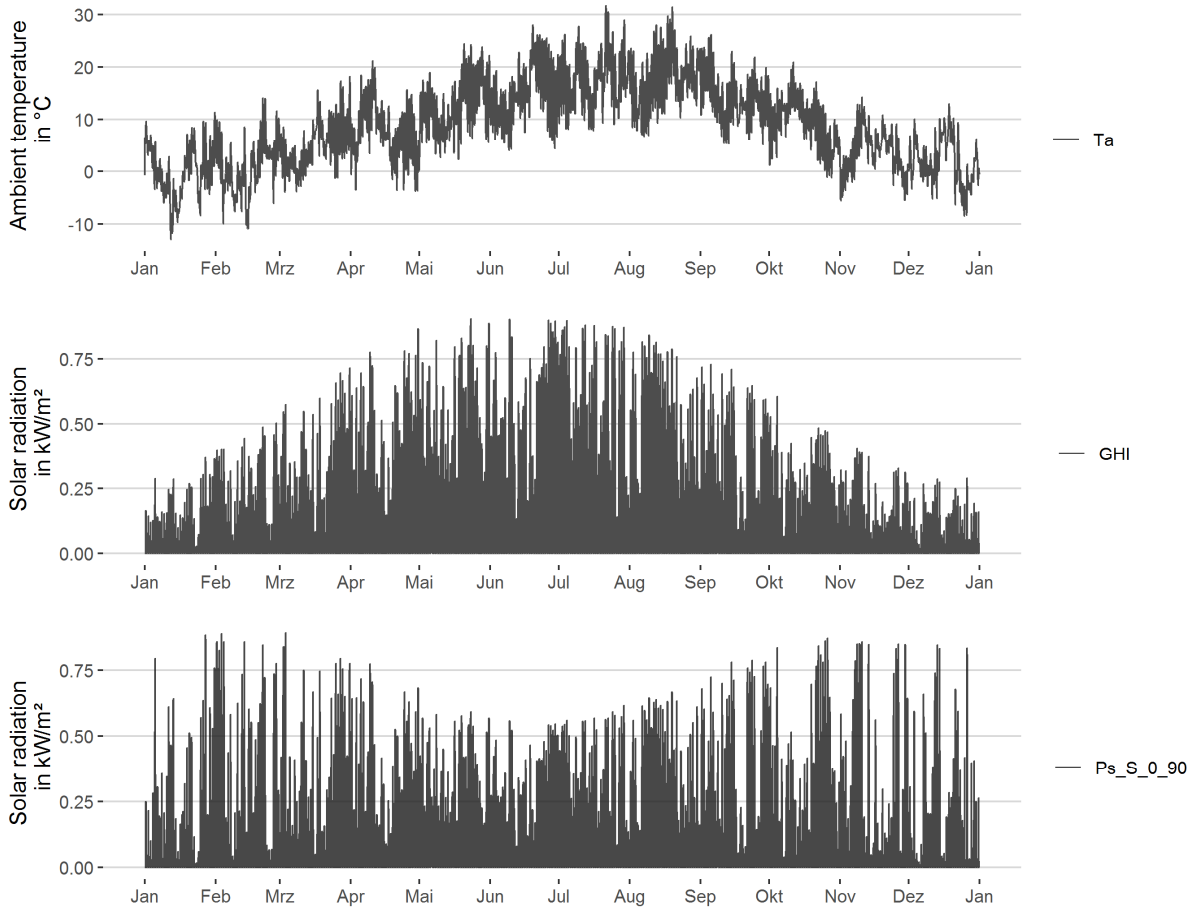


Figure B.1: Hourly values of ambient temperature (upper plot) and solar radiation (lower plot) used for TRNSYS simulations and parameter estimation [54]. For solar radiation, both global horizontal irradiance (GHI) and total solar radiation on the southern vertical surface (Ps_S_0_90) are shown.

Appendix C: RC-model formulation

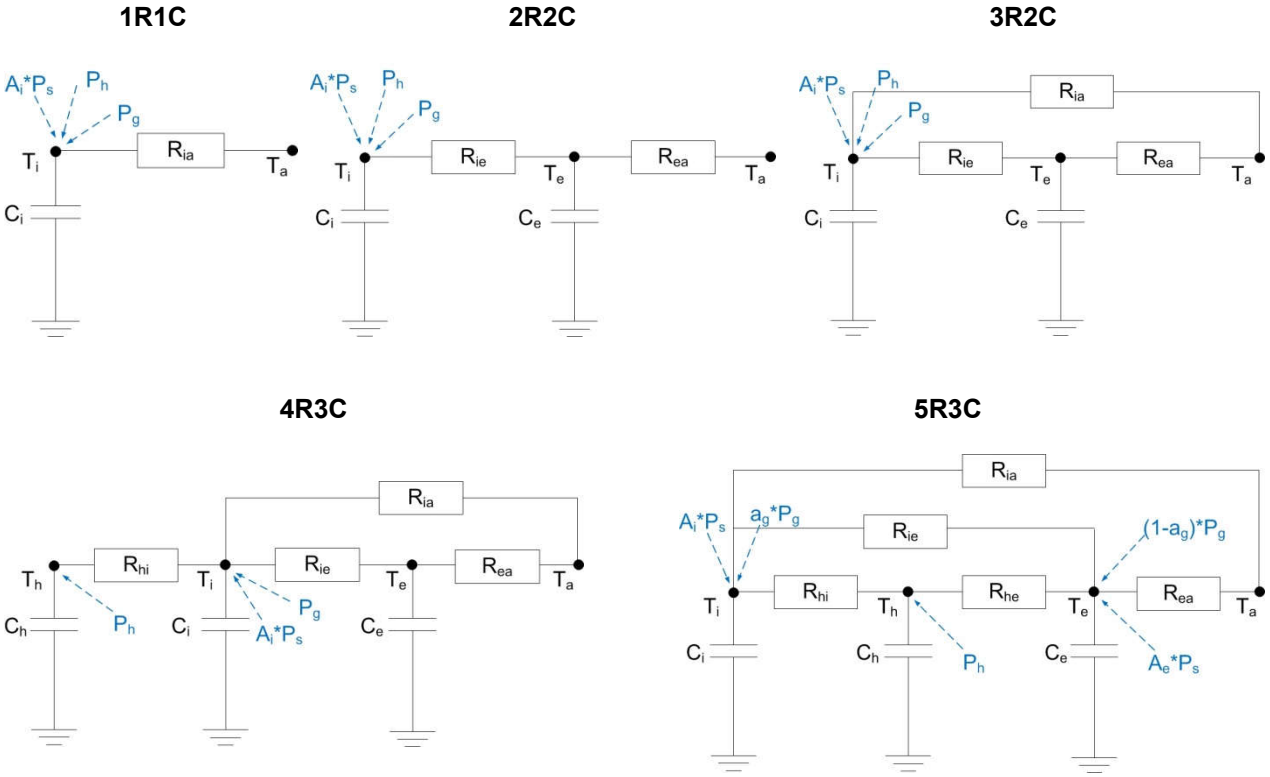


Figure C.1: RC-network representations of the examined building models

Table C.1: Abbreviations used in the RC representations

Code	Description	Unit
T_i	Indoor air temperature	°C
T_e	Temperature of building envelope	°C
T_h	Temperature of heaters	°C
T_a	Ambient temperature	°C
P_h	Heating power	kW
P_g	Internal heat gains	kW
P_s	Solar radiation	kW/m²
R_{ia}	Thermal resistance between interior and the ambient	°C/kW
R_{ie}	Thermal resistance between interior and building envelope	°C/kW
R_{ea}	Thermal resistance between building envelope and the ambient	°C/kW
R_{he}	Thermal resistance between heaters and building envelope	°C/kW
R_{hi}	Thermal resistance between heaters and interior	°C/kW
C_i	Capacitance of interior	kWh/°C
C_e	Capacitance of building envelope	kWh/°C
C_h	Capacitance of heaters	kWh/°C
A_i	Effective window area for absorption of solar gains on internal air	m²
A_e	Effective window area for absorption of solar gains on inside surfaces	m²
a_g	Factor for distributing internal heat gains among the nodes	-
ω	Standard Wiener processes	-
σ	Incremental variance of the Wiener process	-
ε	Gaussian white noise process	-

839 Table C.2: System equations of the grey-box models

Model	System equations	
1R1C	$dT_i = \left[1/(C_i * R_{ia}) * (T_a - T_i) + A_i/C_i * P_s + 1/C_i * \left(P_h + P_g\right)\right]dt + \sigma_i d\omega_i$	Eq. (C.1)
2R2C	$dT_i = \left[1/(C_i * R_{ie}) * (T_e - T_i) + A_i/C_i * P_s + 1/C_i * \left(P_h + P_g\right) \right]dt + \sigma_i d\omega_i$	Eq. (C.2)
	$dT_e = [1/(C_e * R_{ie}) * (T_i - T_e) + 1/(C_e * R_{ea}) * (T_a - T_e)]dt + \sigma_e d\omega_e$	Eq. (C.3)
3R2C	$dT_i = \left[1/(C_i * R_{ie}) * (T_e - T_i) + 1/(C_i * R_{ia}) * (T_a - T_i) + A_i/C_i * P_s + 1/C_i * \left(P_h + P_g\right) \right]dt + \sigma_i d\omega_i$	Eq. (C.4)
	$dT_e = [1/(C_e * R_{ie}) * (T_i - T_e) + 1/(C_e * R_{ea}) * (T_a - T_e)]dt + \sigma_e d\omega_e$	Eq. (C.5)
4R3C	$dT_i = \left[1/(C_i * R_{hi}) * (T_h - T_i) + 1/(C_i * R_{ie}) * (T_e - T_i) + 1/(C_i * R_{ia}) * (T_a - T_i) + A_i/C_i * P_s + 1/C_i * P_g \right]dt + \sigma_i d\omega_i$	Eq. (C.6)
	$dT_h = [1/(C_h * R_{hi}) * (T_i - T_h) + 1/C_h * P_h]dt + \sigma_h d\omega_h$	Eq. (C.7)
	$dT_e = [1/(C_e * R_{ie}) * (T_i - T_e) + 1/(C_e * R_{ea}) * (T_a - T_e)]dt + \sigma_e d\omega_e$	Eq. (C.8)
5R3C	$dT_i = \left[1/(C_i * R_{hi}) * (T_h - T_i) + 1/(C_i * R_{ie}) * (T_e - T_i) + 1/(C_i * R_{ia}) * (T_a - T_i) + A_i/C_i * P_s + a_g/C_i * P_g \right]dt + \sigma_i d\omega_i$	Eq. (C.9)
	$dT_h = [1/(C_h * R_{hi}) * (T_i - T_h) + 1/(C_h * R_{he}) * (T_e - T_h) + 1/C_h * P_h]dt + \sigma_h d\omega_h$	Eq. (C.10)
	$dT_e = [1/(C_e * R_{ie}) * (T_i - T_e) + 1/(C_e * R_{ea}) * (T_a - T_e) + 1/(C_e * R_{he}) * (T_h - T_e) + A_e/C_e * P_s + (1 - a_g)/C_e * P_g]dt + \sigma_e d\omega_e$	Eq. (C.11)

840

841 Table C.3: Observation equation of the grey-box models

Observation equation

$T_i = yT_i + \varepsilon$ Eq. (C.12)

Appendix D: Estimated parameters of the RC-models

Table D.1: Estimated parameters of the 3R2C model for building types A to I with corresponding RMSE for the simulated indoor air temperature

Building type	A_i	C_e	C_i	R_{ea}	R_{ia}	R_{ie}	RMSE Test Data1	RMSE Test Data 2
SFH A Var1	6.98	25.62	2.53	1.03	7.71	0.39	0.93	1.01
SFH A Var2	2.17	20.72	2.56	6.92	7.75	0.37	0.65	0.95
SFH A Var3	1.45	20.72	2.56	15.14	19.22	0.99	0.40	0.59
SFH B Var1	3.12	16.73	1.82	1.88	9.91	0.43	0.94	1.07
SFH B Var2	2.60	13.48	1.98	8.31	9.92	0.78	0.51	0.69
SFH B Var3	0.97	13.42	1.98	17.65	24.77	1.09	0.50	0.86
SFH C Var1	7.34	28.64	3.02	1.11	5.61	0.25	0.82	0.83
SFH C Var2	3.67	28.69	3.16	4.96	5.65	0.19	0.62	0.93
SFH C Var3	2.78	28.65	3.51	7.31	19.65	0.59	0.91	0.59
SFH D Var1	2.58	13.11	1.27	2.26	15.52	0.47	0.85	1.02
SFH D Var2	1.73	10.51	1.27	7.64	23.10	0.26	0.72	1.36
SFH D Var3	0.93	10.51	1.27	19.94	41.75	0.79	0.34	0.66
SFH E Var1	3.79	14.31	1.66	2.11	11.71	0.35	0.89	1.50
SFH E Var2	1.91	11.47	1.68	5.86	17.43	0.30	0.46	0.99
SFH E Var3	1.07	11.47	1.68	14.68	29.27	0.73	0.81	0.99
SFH F Var1	4.80	20.42	1.98	2.32	9.72	0.29	0.62	1.38
SFH F Var2	2.40	16.40	2.02	6.58	14.50	0.30	0.39	0.83
SFH F Var3	1.72	16.39	2.02	13.26	24.38	0.53	0.35	1.05
SFH G Var1	3.79	21.73	2.03	2.81	9.14	0.36	0.51	0.81
SFH G Var2	1.90	20.41	2.16	12.15	8.08	0.45	0.46	0.70
SFH G Var3	1.05	20.41	2.16	16.09	31.86	0.81	0.32	0.76
SFH H Var1	4.16	15.63	1.71	3.72	13.70	0.38	0.50	0.79
SFH H Var2	2.88	14.21	1.71	5.39	28.29	0.33	0.37	1.14
SFH H Var3	1.79	14.21	1.71	14.89	28.69	0.56	0.36	0.41
SFH I Var1	4.54	11.53	1.42	4.89	20.51	0.57	0.36	0.80
SFH I Var2	3.68	11.53	1.42	7.38	20.47	0.47	0.49	0.88
SFH I Var3	2.34	11.53	1.42	15.73	34.48	1.04	0.66	0.59

Table D.2: Estimated parameters of the 4R3C models for building types J to L with corresponding RMSE for the simulated indoor air temperature

Building type	A_i	C_e	C_h	C_i	R_{ea}	R_{hi}	R_{ia}	R_{ie}	RMSE Test Data1	RMSE Test Data 2
SFH J Var1	1.42	10.40	1.44	1.60	12.99	4.13	12.32	0.56	0.67	0.98
SFH J Var2	1.98	10.40	1.93	1.60	12.70	3.75	12.32	0.56	0.28	0.51
SFH J Var3	1.42	10.41	1.97	1.60	15.25	3.99	30.75	0.52	0.33	0.52
SFH K Var1	2.94	12.52	2.66	2.76	11.18	2.56	7.20	0.48	0.88	0.76
SFH K Var2	2.94	12.53	2.48	2.76	12.18	3.59	7.59	0.58	0.87	0.67
SFH K Var3	2.10	12.53	1.47	2.76	22.96	5.18	18.44	0.48	0.53	1.09
SFH L Var1	2.94	12.52	2.50	2.76	10.28	2.99	7.12	0.46	0.60	0.81
SFH L Var2	2.94	12.53	1.84	2.76	14.47	4.48	8.39	0.54	0.91	0.56
SFH L Var3	2.10	12.53	1.43	2.76	22.96	5.18	18.51	0.49	0.59	1.05